SHIMADZU
Excellence in Science

Quadrupole Time-of-Flight
Liquid Chromatograph Mass Spectrometer

# LCMS-9030


# Effortless performance

The LCMS-9030 quadrupole time-of-flight (Q-TOF) mass spectrometer integrates the world's fastest and most sensitive quadrupole technology with TOF architecture. It delivers high resolution accurate-mass detection with incredibly fast data acquisition for routine applications.

- **Greater accuracy and higher sensitivity**
- **Identify and quantify more compounds with greater confidence**
- **Small footprint**

DESIGN AWARD 2019

**www.shimadzu.eu**/effortless-performance

Received: 24 March 2021 | Revised: 21 June 2021 | Accepted: 21 June 2021

DOI: 10.1002/rcm.9151

RESEARCH ARTICLE

Rapid Communications in Mass Spectrometry WILEY

# Direct infusion and ultra-high-performance liquid chromatography/electrospray ionization tandem mass spectrometry analysis of phospholipid regioisomers

Mikael Fabritius | Baoru Yang

Food Chemistry and Food Development, Department of Biochemistry, University of Turku, Turku, Finland

**Correspondence**
B. Yang, Food Chemistry and Food Development, Department of Life Technologies, University of Turku, FI-20014 Turku, Finland.
Email: baoru.yang@utu.fi

**Funding information**
Academy of Finland, Grant/Award Number: 310982; University of Turku Graduate School

**Rationale:** Phospholipids are important components of cell membranes that are linked to several beneficial health effects such as increasing plasma HDL cholesterol levels, improving cognitive abilities and inhibiting growth of colon cancer. The role of phospholipid (PL) regioisomers in all these health effects is, however, largely not studied due to lack of analytical methods.

**Methods:** Electrospray ionization mass spectrometry in negative mode produces structurally informative fragment ions resulting from differential dissociation of fatty acids (FAs) from the *sn*-1 and *sn*-2 positions, primarily high-abundance $[RCOO]^-$ ions. The fragment ion ratios obtained with different ratios of regiopure phospholipid reference compounds were used to construct calibration curves, which allow determination of regioisomeric ratios of an unknown sample. The method was developed using both direct infusion mass spectrometry (MS) and ultra-high-performance liquid chromatography and hydrophilic interaction liquid chromatography mass spectrometry (UHPLC-HILIC-MS).

**Results:** The produced calibration curves have high coefficients of determination ($R^2$ >0.98) and the fragment ion ratios in replicate analyses were very consistent. A test mixture containing 60/40% ratios of all available regioisomer pairs was analyzed to test and validate the functionality of the calibration curves. The results were accurate and reproducible. However, regioisomeric quantification of certain chromatographically overlapping compounds is restricted by the relatively wide window in precursor ion selection of the MS instrument used.

**Conclusions:** This method establishes a framework for analysis of phospholipid regioisomers. Specific regioisomers can be quantified using the existing data, and method development will continue with improving chromatographic separation and exploring the fragmentation patterns and efficiencies of different PL classes and FA combinations, ultimately to refine this method for routine analysis of natural fats and oils.

## 1 | INTRODUCTION

Phospholipids (PLs) are a group of polar compounds that typically consist of two fatty acid (FA) molecules and a polar head group attached to the glycerol backbone. FAs are esterified to the *sn*-1 and *sn*-2 positions of the glycerol carbon chain and the polar head group is connected to the *sn*-3 position via a phosphodiester bond. PLs are divided into different classes based on the polar head group, the most common examples being phosphatidylcholine (PC), phosphatidylethanolamine (PE), phosphatidylinositol (PI) and phosphatidylserine (PS). The combination of different FA substituents and polar head groups potentially results in hundreds of different PL molecular species in natural samples. Additionally, changing the relative positions of FAs on the glycerol backbone results in regioisomerism, further increasing the potential complexity. Sphingomyelins (SMs) containing an amino alcohol group, while classified as sphingolipids, are often reported among phospholipids.

PLs are a vital structural component of cell membranes, arranged as lipid bilayers, and there are well-documented beneficial effects of dietary PLs. Milk fat globule membrane with high PL content[1] and PLs of marine origin[2,3] have been linked to growth inhibition of colon cancer. Oral intake of PC has been shown to improve learning and memory of people with cognitive disorders[4] and certain fish oils rich in PLs, such as krill oil, have similar effects possibly due to better incorporation of omega-3 FAs into membranes than triacylglycerol (TAG)-rich fish oils.[5] Dietary PLs may have a beneficial effect on plasma lipid and lipoprotein levels by increasing high-density lipoproteins and reducing low-density lipoproteins, thus improving blood cholesterol levels.[6,7] PLs are also reported to reduce rheumatoid arthritis symptoms[8] and may have a positive effect on immune response.[9] The *sn*-positioning of FAs in TAGs, especially palmitic acid, has been shown to affect absorption of FAs, influencing the formation of insoluble calcium soaps that are excreted.[10–12] However, while the evidence suggests that PLs have beneficial health effects, the significance of different PL structural isomers in the diet is still largely an unanswered question due to the lack of commercially available regiospecific standards and routine analytical methods.

Traditional methods for phospholipid analysis include thin-layer chromatography (TLC)[13] and high-performance liquid chromatography (HPLC) coupled to an evaporative light scattering detector (ELSD).[14,15] While these methods can quantify PLs on the class level, they provide no information on individual molecular species. The popularity of mass spectrometric applications for PL analysis has increased greatly during the past decade due to easier profiling of PL molecular species and potential for structural analysis with tandem mass spectrometry (MS/MS). Hydrophilic interaction liquid chromatography (HILIC) is the most commonly used technique for separation of PL classes, where the separation occurs primarily based on the polar head group of the PL compound, with electrospray ionization (ESI) as the preferred ionization mode for MS applications.[15–19] Direct infusion without chromatography has also been used for PL class and molecular species identification.[20]

Previous studies suggest that PLs produce structurally informative fragments in negative ionization mode. FA anions $[RCOO]^-$ cleaved from the *sn*-1 or *sn*-2 positions are observed from fragmentation of PC, PE, PI and PS, which allows the structural characterization of the precursor ion.[21–25] The fragmentation pathways for these PL classes have also been explored previously.[22,25–30] While several studies have identified FAs in PL molecular species,[17,21–25,30,31] the regioisomeric distribution of *sn*-1 and *sn*-2 FAs in natural samples still remains mostly unexplored. An analytical method for lysophosphatidic acid regioisomers has been developed utilizing adequate chromatographic separation of the *sn*-1 and *sn*-2 regioisomers.[32] Another method has been developed for analysis of PC regioisomers based on partial separation of the regioisomers with reversed-phase (RP) chromatography and identification of the front and tail ends of the split peaks with ESI-MS/MS.[33] A different type of approach for PL regioisomer analysis has been reported, utilizing minor differences in the retention times of PL regioisomers and the change in the $[RCOO]^-$ fragment ion ratios as the PL regioisomers of interest are coeluting.[34] Differential ion mobility spectrometry (DMS) with electron-impact excitation of ions from organics (EIEIO) mass spectrometry has also been applied to comprehensive identification of lipids, including PL regioisomers.[35] DMS separates ions in the gas phase based on small differences in their structures, which allows one additional orthogonal separation step for isobaric compounds and has the future potential to be very useful in structural characterization of lipids. It does, however, require somewhat more specialized and expensive instrumentation compared with ESI-MS/MS systems.

In this study we present an accurate and reproducible method for calculating specific PL regioisomers utilizing calibration curves based on the product ion ratios of PL reference standard compounds. The method was tested with both direct infusion and HILIC/ESI-MS/MS and will provide a basis for further method development and optimization for complex natural samples.

## 2 | MATERIALS AND METHODS

### 2.1 | Abbreviations and nomenclature

Abbreviations for individual FAs are denoted as 20:4 = arachidonic, 18:3 = α-linolenic, 18:2 = linoleic, 18:1 = oleic, 18:0 = stearic, 16:1 = palmitoleic, 16:0 = palmitic and 14:0 = myristic acid. ACN: DB = the ratio of the number of acyl carbons/number of double bonds. Regioisomers of PLs are denoted as *PL A/B*, where A and B are different FAs esterified to the *sn*-1 and *sn*-2 positions on the glycerol backbone, respectively, and *PL* indicates the phospholipid class. For example, *sn*-1-palmitoyl-*sn*-2-oleoyl-glycero-*sn*-3-phosphatidylcholine is denoted as PC 16:0/18:1. PLs with known FAs, but unknown *sn*-positioning, are denoted as *PL A_B*. No distinction is made between the locations of double bonds in FA carbon chains.

## 2.2 | Materials

HPLC-grade chloroform and LC/MS grade methanol were purchased from VWR International (Radnor, PA, USA). LC/MS grade acetonitrile and water were purchased from Fisher Chemical (Waltham, MA, USA). LC/MS grade ammonium formate and formic acid were purchased from Sigma-Aldrich (St Louis, MO, USA). All regiospecific PL standards were purchased from Avanti Polar Lipids (Alabaster, AL, USA). Regioisomeric pairs consisted of PC 14:0/16:0 / PC 16:0/14:0; PC 14:0/18:0/ PC 18:0/14:0; PC 16:0/18:0/ PC 18:0/16:0; PC 16:0/18:1 / PC 18:1/16:0; PC 16:0/18:2/ PC 18:2/16:0; PC 16:0/18:3/ PC 18:3/16:0; PC 16:0/20:4/ PC 20:4/16:0; PE 16:0/18:1/PE 18:1/16:0 and PS 16:0/18:1/PS 18:1/16:0. Natural PI (from soybean) and SM (from egg) extracts were purchased from Larodan (Malmö, Sweden). Additionally, non-regiospecific monoacid PC, PE and PS reference standards for initial chromatographic method development were purchased from Avanti Polar Lipids. For a complete list of all used reference standards, see Table S1 (supporting information).

## 2.3 | Sample preparation

All PL reference standard compounds were shipped in $CHCl_3$ solution. All subsequent dilutions were made with $CHCl_3$/MeOH (2:1, v/v). Five mixtures of the PL regioisomer pairs at different ratios (100:0, 75:25, 50:50, 25:75 and 0:100) were prepared in order to construct the calibration curves. The final concentration of each mixture was a combined total of 10 μg/mL. A test mixture containing all regiospecific pairs at 60:40% ratios with a total concentration of 10 μg/mL for each pair was prepared for method validation. Reference compounds were analyzed without further pretreatment and filtered with a 0.2 μm Acquity column in-line filter (Waters Corp., Milford, MA, USA) during the analysis right before being introduced into the ion source.

## 2.4 | UHPLC/MS/MS system and analysis conditions

PL regioisomers were analyzed either with the direct infusion MS/MS or UHPLC/MS/MS system. The UHPLC system consisted of a Cortecs UPLC HILIC 1.6 μm column ((2.1 × 150 mm; Waters Corp.) and an Elute HPG 1300 pump unit (Bruker Corp., Billerica, MA, USA). The binary solvent gradient consisted of (A): $H_2O$/ACN (80:20, v/v) with 5 mM ammonium formate and (B): ACN/$H_2O$ (95:5, v/v) with 5 mM ammonium formate. A stock solution of 100 mM ammonium formate in $H_2O$ (pH 3.0, adjusted with formic acid) was used when preparing the mobile phase solvents. The mobile phase gradient was as follows: initial solvent composition was 6% A, 6 to 9% A (0–20 min), 9 to 20% A (20–40 min), 20 to 70% A (40–41 min), held at 70% A (41–48 min), 70 to 6% A (48–49 min) and held at 6% A (49–65 min). Total solvent flow rate was 0.15 mL/min from 0 to 41 min, then changed to 0.3 mL/min during the column flushing and equilibration phase from 41 to 62 min and changed back to 0.15 mL/min at 62 min before the next injection. The injection volume for all samples was 2 μL. Direct infusion of the PL standards was performed using a syringe pump (model 300; New Era Pump Systems, Farmingdale, NY, USA) with a T-split connecting the syringe pump flow to the LC mobile phase flow. The syringe pump flow was set at 5 μL/min and the LC flow rate at 0.15 mL/min 15% A/85% B.

MS/MS analyses were performed with an Impact II quadrupole time-of-flight (qTOF) tandem mass spectrometer (Bruker Corp.) using an electrospray ionization (ESI) source. The capillary voltage was set at 3500 V and the end plate offset at 500 V. The nebulizer gas pressure was set at 2 bar, drying gas flow rate at 8 L/min and drying gas temperature was at 300°C. The collision energy was set at 40 eV for all studied samples. For direct infusion analyses product ion scans were used for the selected precursor ions of the PL reference standards and the data was recorded from a 10 s window after the syringe pump flow had stabilized. For the UHPLC/MS/MS analyses a non-targeted approach (autoMS/MS) was used, which selects precursor ions for fragmentation when the intensity exceeds a set threshold. The precursor ion intensity threshold for autoMS/MS fragmentation was set at 600 counts, which was slightly above background noise levels. The maximum number of simultaneous product ion scans was set at five, meaning that the autoMS/MS prioritizes fragmentation of the five most abundant ions at any given time. MS scan time was 0.25 s and autoMS/MS total cycle time for five consecutive scans was 1.4 s.

# 3 | RESULTS AND DISCUSSION

## 3.1 | Method optimization

Initial testing was performed in positive ionization mode to confirm the previous observations of lack of structurally informative fragment ions.[23–25] All subsequent analyses were performed using negative ionization mode. Depending on class, PLs were detected as deprotonated molecular $[M - H]^-$ or as formate adduct $[M + HCOO]^-$ ions. Optimization of MS and MS/MS instrument parameters was performed with direct infusion of PC 16:0/18:1, PE 16:0/18:1 and PS 16:0/18:1 reference standards. Capillary voltage, end plate offset voltage, nebulizer gas pressure and drying gas flow rate were manually optimized with the goal of having the highest possible precursor ion sensitivity. Lowering the drying gas flow rate and increasing the temperature showed improved sensitivity compared with default values. Quadrupole settings were adjusted with a tuning function, which automatically tests the settings one by one and shows a graph of the intensity response with different values tested. For each setting, the value producing the highest amount of precursor ions was selected. All optimized MS settings can be found in Table S2 (supporting information). Effects of optimization on mass resolution were negligible for the purposes of this study. The collision

energy for MS/MS fragmentation was tested in the 10–60 eV range. In most cases a collision energy of 40 eV produced abundant FA ions $[RCOO]^-$ and smaller quantities of lysophospholipid-like fragment ions. Both of these can be used for structural analysis, but FA ions were the preferable option due to higher sensitivity. The collision energy did not seem to have a major effect on the relative proportions of these structurally informative fragment ions, resulting in the primary criterion for collision energy selection being the highest possible abundance of these fragment ions.

The primary goal of the liquid chromatographic method optimization was good PL class separation. Non-regiospecific monoacid PL standards were used for initial chromatography optimization. The gradient was further optimized for increased molecular species separation, which to some degree worked for PC, PE and SM, but in general is quite challenging for the HILIC column due to the separation being mostly affected by the polar head group and only to a lesser extent by the attached FAs. All tested PS standards exhibited poor peak shape, which did not seem to be affected by changing the gradient or flow rate, but the PS class cluster was reasonably well separated from other PL classes (Figure 1). Compared with a more traditional timed multiple reaction monitoring (MRM) method, autoMS/MS allows for a more robust analytical method that does not require the user to know beforehand what precursor ions to monitor and is useful when analyzing complex natural samples. HILIC columns are typically quite sensitive and highly susceptible to shifting retention times over subsequent analyses. This was also the case during our testing. There was noticeable peak drifting in our early method development, and only after extensive testing and long equilibration phase with higher flow rate, was the effect somewhat reduced. Subsequent analyses during a single day were fairly consistent, but noticeable weekly variance in retention times was observed. The autoMS/MS is a good tool in mitigating the effects of shifting retention times as it does not require strict time windows for specific precursor ions. Additionally, the user can manually add a list of precursor ions that the autoMS/MS prioritizes over others, or exclude certain ions, which reduces the effect of high-abundance background ion interference.

## 3.2 | Ionization and fragmentation of different PL classes

### 3.2.1 | Phosphatidylcholine

PCs produced abundant $[M + HCOO]^-$ ions and lesser quantities of $[M + HCOO + 68]^-$, $[M + HCOO + 136]^-$ and other similar higher mass adducts 68 Da apart from each other (see Figure 2a for more information). The 68 Da mass difference likely corresponds to sodium formate $(HCOONa)_n$ cluster adduct ions. While sodium is not intentionally present in the mobile phase or sample, it is commonly described as a contaminant that can originate for example from glassware or solvents, and is difficult to get rid of.[36] Only the $[M + HCOO]^-$ ions were used for quantification purposes and subsequent fragmentation. Collision-induced dissociation (CID) at 40 eV collision energy produced FA ions $[R_1COO]^-$ and $[R_2COO]^-$ in abundant quantities (Figure 3a). For PC 16:0/18:1, the 18:1 FA ion was the most abundant and the 16:0 ion had roughly 30% intensity of the 18:1 ion (Figure S1, supporting information). With the other regioisomer PC 18:1/16:0, the ratios of FA ions were practically reversed, indicating that the FA is more easily cleaved from the *sn*-2 position. This fragmentation behavior has been reported by others as well. Lísa et al[37] and Han et al[38] have also analyzed PC 16:0/18:1, both studies showing very similar $[RCOO]^-$ fragment ion ratios using ESI-MS/MS in negative ionization mode compared with our study. A similar pattern was observed with all other investigated PC regioisomer pairs. While there were some differences in the FA ion ratios with PCs containing different FAs, the *sn*-2 FA always produced the most abundant ions. Preference of FA cleavage from the *sn*-2 position has also been documented previously and it was also noted that the ratio is dependent on the FA chain length and degree of saturation.[22] This FA ion ratio can be used to construct calibration curves for the reference standards, allowing quantification of regioisomer ratios of an unknown sample. In addition to the FA ions, lower quantities of other higher mass ions tentatively identified as $[M + HCOO - RCOOH - 42]^-$ and $[M + HCOO - RCOOH - 60]^-$ were detected. The ratios of $[M + HCOO - RCOOH - 42]^-$ ions followed similar behavior compared with $[RCOO]^-$ ions, where

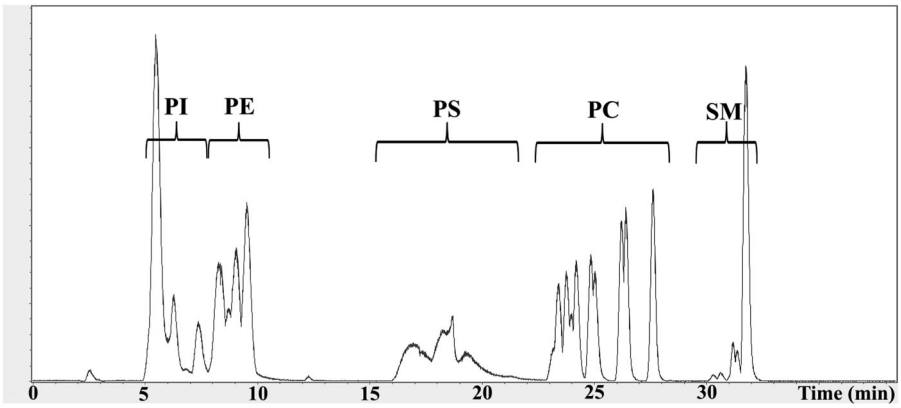


**FIGURE 1** Chromatogram of a PL reference standard mixture, PC (12:0/12:0, 14:0/14:0, 14:1/14:1, 16:0/16:0, 16:1/16:1, 18:0/18:0, 18:1/18:1, 18:2/18:2, 18:3/18:3, 20:0/20:0 and 22:0/22:0; 10 μg/mL each), PE (14:0/14:0, 16:0/16:0, 18:0/18:0 and 18:1/18:1; 10 μg/mL each), PS (14:0/14:0, 16:0/16:0, 18:0/18:0 and 18:1/18:1; 10 μg/mL each) and natural extracts of PI from soybean and SM from egg (20 μg/mL each)

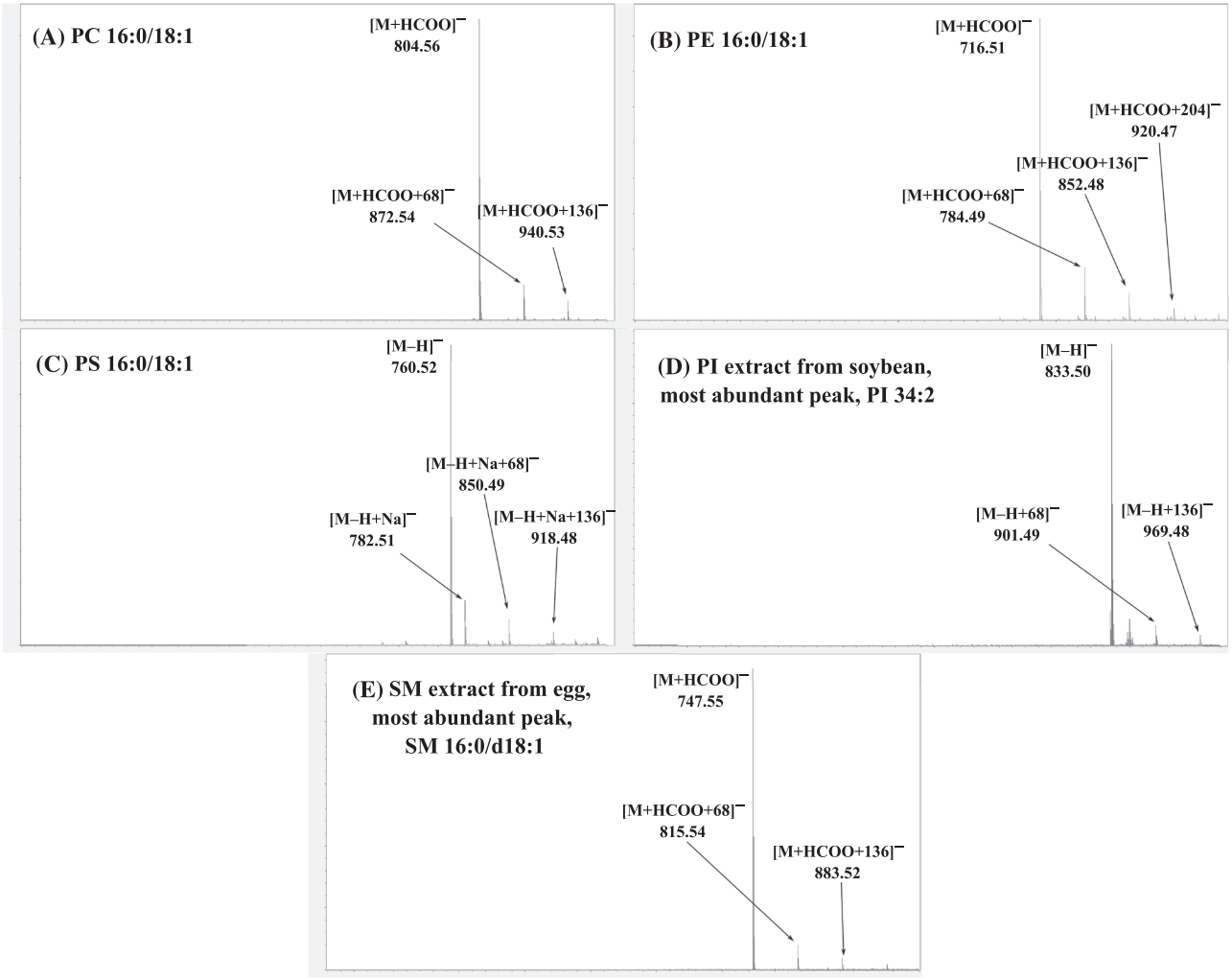


**FIGURE 2** Ionization and adduct formation of different PL compounds: (a) PC 16:0/18:1, (b) PE 16:0/18:1, (c) PS 16:0/18:1, (d) PI extract from soybean, and (e) SM extract from egg

$[M + HCOO - R_2COOH - 42]^-$ was always more abundant than $[M + HCOO - R_1COOH - 42]^-$. While the abundance of $[M + HCOO - RCOOH - 42]^-$ ions is significantly lower compared with FA ions, it is possible to construct another set of calibration curves which can be used for quantification independently from the FA ion calibration curves. There was also a relatively high abundance of $[M + HCOO - 60]^-$ ions detected in the MS/MS spectra, but these are not structurally informative.

### 3.2.2 | Phosphatidylethanolamine

PEs were mainly detected as $[M–H]^-$ ions. Similarly to PCs, smaller quantities of possible sodium formate adduct cluster ions 68 Da apart from each other were detected in the MS spectra (Figure 2b). Abundant FA ions $[R_1COO]^-$ and $[R_2COO]^-$ were detected in the MS/MS spectra and the ratios of FA ions behaved very similarly compared with PCs and can be used for structural characterization (Figure 3b). Han et al[38] reported that fragmentation of PE 16:0/18:1 produced *sn*-2 FA fragments at a ratio of approximately 3:1 compared with *sn*-1 FA fragments, a result very similar to our own findings. They also observed that this ratio close to 3:1 was true for several other investigated PEs (16:0/18:2, 16:0/20:4, 18:0/18:1, 18:0/18:2, 18:0/20:4 and 18:1/20:4) with FAs containing up to 20 carbon atoms. However, the ratio was dramatically different (1–1.5:1) when one of the FAs was highly polyunsaturated with at least 22 carbon atoms.[38]

Additionally, minor quantities of higher mass fragments were detected in our analyses, which were identified as $[M - H - RCOOH]^-$ and $[M - H - R'CH{=}C{=}O]^-$ based on the fragmentation pathways explored in earlier studies.[30] The fragmentation behavior of the $[M - H - RCOOH]^-$ ions was similar compared with the $[M + HCOO - RCOOH - 42]^-$ fragments from PCs and the ratios were logical as the abundance of $[M - H - R_2COOH]^-$ was higher than $[M - H - R_1COOH]^-$, again indicating that the FAs are more easily cleaved from the *sn*-2 position. In addition to the FA fragment ions, also $[M - H - RCOOH]^-$ could be used for structural characterization when the sensitivity allowed it.

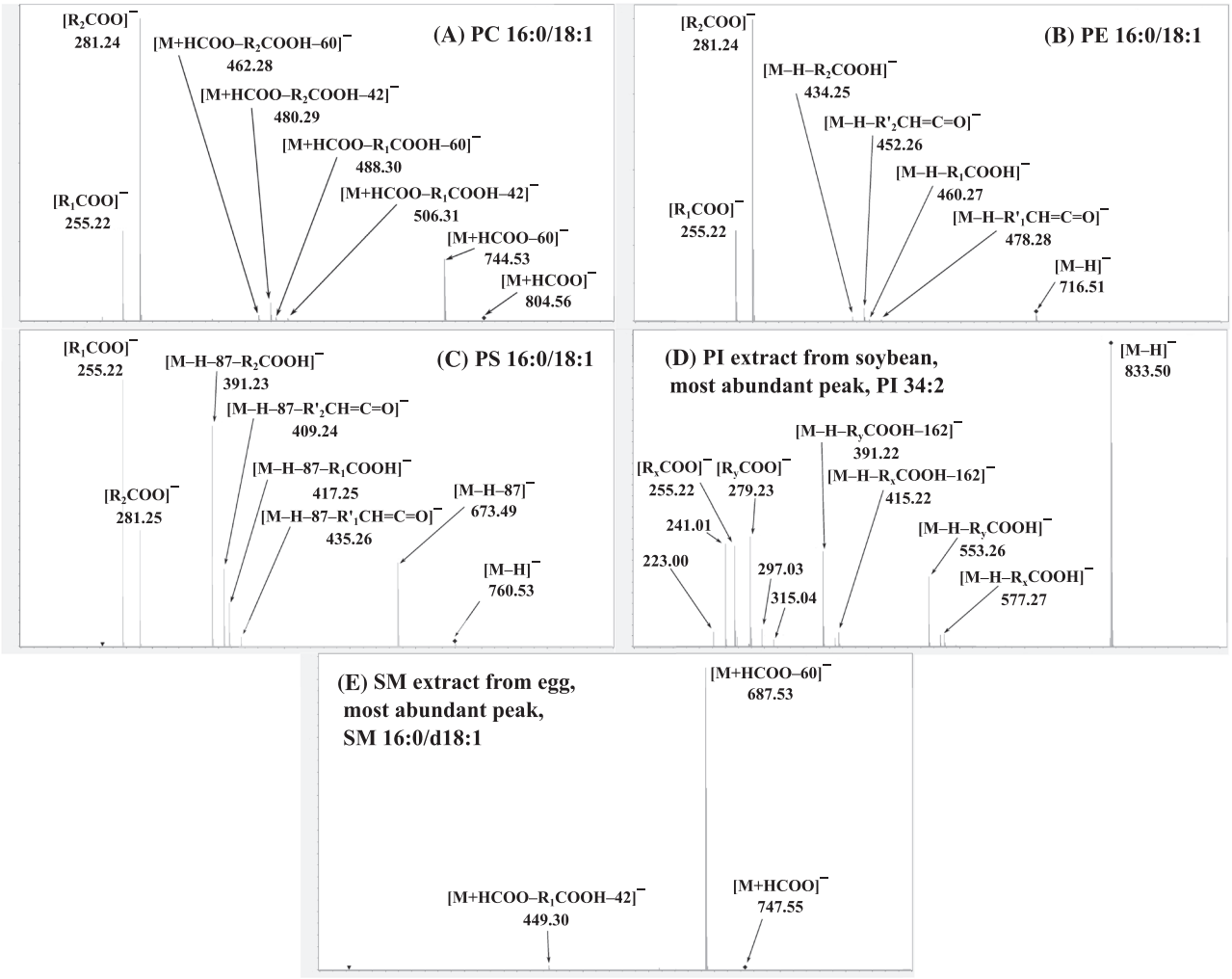


**FIGURE 3** Fragmentation of PL test samples showing the *m/z* ratio of each major fragment ion and tentative identifications: (a) PC 16:0/18:1, (b) PE 16:0/18:1, (c) PS 16:0/18:1, (d) PI extract from soybean (most abundant peak, PI 34:2 molecular species), and (e) SM extract from egg (most abundant peak, SM 16:0/d18:1)

### 3.2.3 | Phosphatidylserine

The PS 16:0/18:1 reference standard produced abundant $[M - H]^-$ ions and smaller quantities of sodium formate adduct cluster ions (Figure 2c). For the purposes of regioisomer analysis, only the fragments of the $[M - H]^-$ ions were investigated. Again, CID at 40 eV produced abundant FA ion fragments which can be used for quantification, but the ratios were noticeably different compared with the PC and PE reference standards with the same FA configuration (Figure 3c). With PS 16:0/18:1, the 16:0 FA fragment from the *sn*-1 position was more abundant than the 18:1 FA fragment from the *sn*-2 position. Other product ions resulting from neutral loss of the serine group $[M - H - 87]^-$, neutral losses of serine and acyl ketenes $[M - H - 87 - R'CH{=}C{=}O]^-$ and neutral losses of serine and FAs $[M - H - 87 - RCOOH]^-$ were detected as identified earlier.[22] The $[M - H - 87 - RCOOH]^-$ ions were nearly as abundant as the FA ion fragments, also enabling regioisomeric quantification. However, the relative proportions of $[R_1COO]^-/[R_2COO]^-$ and $[M - H - 87 - R_1COOH]^-/[M - H - 87 - R_2COOH]^-$ were somewhat unexpected compared with PC and PE; while the $[R_1COO]^-$ ions were more abundant than $[R_2COO]^-$ ions, the $[M - H - 87 - R_2COOH]^-$ ions were more abundant than $[M - H - 87 - R_1COOH]^-$. Based on this information alone it is difficult to determine whether CID favors fragmentation of FAs from the *sn*-1 or *sn*-2 positions within PS molecular species. A similar fragmentation behavior has been documented earlier by Hsu and Turk,[26] where the product ion spectra of the $[M - H]^-$ ion of PS 16:0/18:1 was very similar compared with our current study; the *sn*-1 FA fragment was more abundant than the *sn*-2 FA fragment, and $[M - H - 87 - R_2COOH]^-$ ions were more abundant than $[M - H - 87 - R_1COOH]^-$. Additionally, another study by Larsen et al[23] reported similar fragment ion ratios from PS 18:0/18:1. One possible explanation on the unusual ratios of the fragment ions was given by Hvattum et al,[22] who suggested that PS fragmentation behavior is quite similar to phosphatidic acid (PA), and that the formed $[M - H - 87 - RCOOH]^-$ ions may undergo further

fragmentation processes, resulting in an increased $[R_1COO]^-/[R_2COO]^-$ abundance ratio at higher collision energies. Regardless of which *sn*-position CID favors, it is possible to construct calibration curves using the regiospecific reference standards.

### 3.2.4 | Phosphatidylinositol

For PI we did not have pure reference standards, and for testing we used a commercial PI extract from soybean. The dominating peak in this sample was *m/z* 833.50, which was studied in detail (Figure 2d). The detected ion at *m/z* 833.50 corresponds to the $[M - H]^-$ ion of the PI 34:2 molecular species. In the MS/MS spectra we can see 16:0 and 18:2 FA fragment ions, which corresponds to an ACN/DB ratio of 34:2 (Figure 3d). Additionally, close to the usual *m/z* range of FAs we can see several other unidentified ions, which do not correspond to any FA. Higher mass $[M - H - RCOOH]^-$ and [M – H – RCOOH – 162] fragments were also detected, where the ion at *m/z* 162 is likely the result of cleavage of the inositol group. Hsu and Turk[28] have investigated the fragmentation patterns of PI 16:0/18:2 at 40 eV collision energy, a very similar setup to our experiments. The fragment ion spectra in their study were quite comparable to ours, yielding all of the same structurally informative fragment ions. The $[M - H - RCOOH]^-$ and $[M - H - RCOOH-162]^-$ ions were slightly more abundant in our experiments, but otherwise the relative abundances of the *sn*-1/*sn*-2 fragment ion ratios were similar.[28] Loss of the *sn*-2 FA is reported to be preferential compared with *sn*-1 FA, but, in a similar way to PS, the lysophospholipid-like $[M - H - RCOOH]^-$ and [M – H – RCOOH – 162]$^-$ ions may undergo further fragmentation processes, resulting in a somewhat higher $[R_1COO]^-/[R_2COO]^-$ abundance ratio.[28] While it is not possible to quantify ratios of regioisomers without reference standards and calibration curves, it is possible to qualitatively identify the molecular species based on the FA fragments.

### 3.2.5 | Sphingomyelin

For SM we had a commercial extract from egg for testing purposes instead of a pure reference standard. The SM molecular species in the extract are separated into five distinct peaks in the chromatogram, and clearly the most abundant one is at *m/z* 747.55 (Figure 2e), which corresponds to a $[M + HCOO]^-$ adduct ion of SM 34:1. CID at 40 eV produces a high abundance of $[M - H - 60]^-$ ions and only very low abundance of structurally informative $[M + HCOO - RCOOH-42]^-$ ions (Figure 3e). However, even the low abundance of $[M + HCOO - RCOOH-42]^-$ ions provides useful structural information on the SM molecular species as there is only one FA linked to the amino alcohol group, most commonly sphingosine. By looking at the precursor mass and the $[M + HCOO - RCOOH - 42]^-$ fragment we can determine what the cleaved FA was. In this example, *m/z* 747.55 is identified as containing palmitic acid and sphingosine (SM 16:0/d18:1).

## 3.3 | Determination of PL regioisomer composition

PLs having a maximum of only two different FAs means that while the number of possible combinations is very large, different PL molecular species with the same precursor *m/z* ratio do not have common FAs. For example, the PC 34:1 molecular species could consist of PC 16:0_18:1, PC 16:1_18:0, PC 14:1_20:0, etc. This means that even with the same precursor ion *m/z* ratio, the structurally informative FA fragments do not overlap with each other, and each precursor produces unique fragments, allowing the regioisomeric quantification by using calibration curves.

### 3.3.1 | Calibration curves

The reference standard mixtures consisting of five different concentrations of each PL regioisomer pair were used to construct the calibration curves. The five-point calibration data of the $[RCOO]^-$ fragment ion ratios was fitted to a trendline using the exponential function in Microsoft Excel 2016. The calibration curves are presented in Figure 4 and the coefficient of determination for each curve is very good ($R^2$ >0.99), indicating that there is a very strong correlation between the regioisomeric ratio and the $[RCOO]^-$ fragment ion ratio. As was noted earlier, the $[RCOO]^-$ fragment ratios of the PS reference standards were noticeably different compared with the others, which is also reflected in the calibration curve. All PC and PE reference standards behaved fairly similarly, but there were some differences in the $[RCOO]^-$ fragment ion ratios. The degree of unsaturation in the FAs and the carbon chain length seem to play a role in the fragment ion ratios, influencing the equation to some extent. When comparing the calibration curves of PC 16:0/18:0/ PC 18:0/16:0, PC 16:0/18:1/ PC 18:1/16:0, PC 16:0/18:2/PC 18:2/16:0 and PC 16:0/18:3/PC 18:3/16:0, where the only difference is the degree of saturation in one FA, the presence of more unsaturated FAs seems to cause stronger differentiation in fragmentation of FAs between the *sn*-1 and *sn*-2 positions. In order to establish some general rules for the fragmentation behavior, further investigation is still needed. The mass response and subsequent correction factors for each $[RCOO]^-$ fragment should be established for example by analyzing equimolar concentrations of PLs containing only one type of FA in both *sn*-positions (PC 16:0/16:0, PC 18:1/18:1, PC 18:2/18:2, etc.). By correcting the over- or underrepresented $[RCOO]^-$ ions, it could be possible to adjust the calibration curves to find some patterns that might help in extrapolating additional calibration curves, for which there are no regiospecific reference standards available. Having additional reference standards would of course be very useful; unfortunately, however, they are either not commercially available or extremely expensive to synthesize.

In addition to the $[RCOO]^-$ ions, another set of calibration curves using the lysophospholipid-like fragment ions (PC $[M + HCOO - RCOOH - 42]^-$, PE $[M - H - RCOOH]^-$ and PS $[M - H - RCOOH-87]^-$) was constructed (Figure 5), also with a good coefficient of determination ($R^2$ >0.98) in each case even though their

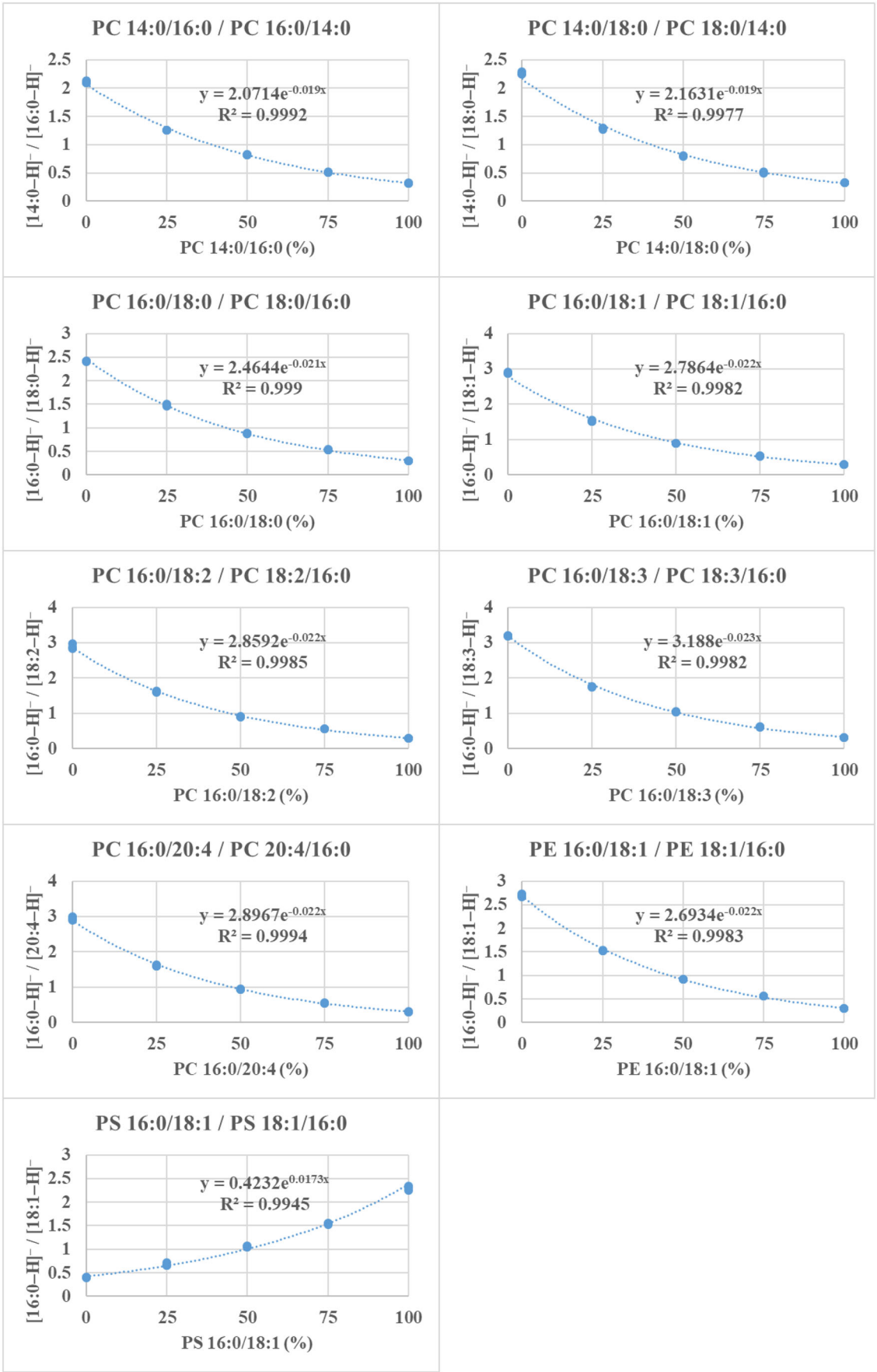


**FIGURE 4** Calibration curves of the regiospecific PL reference standard pairs using $[RCOO]^-$ fragment ion ratios

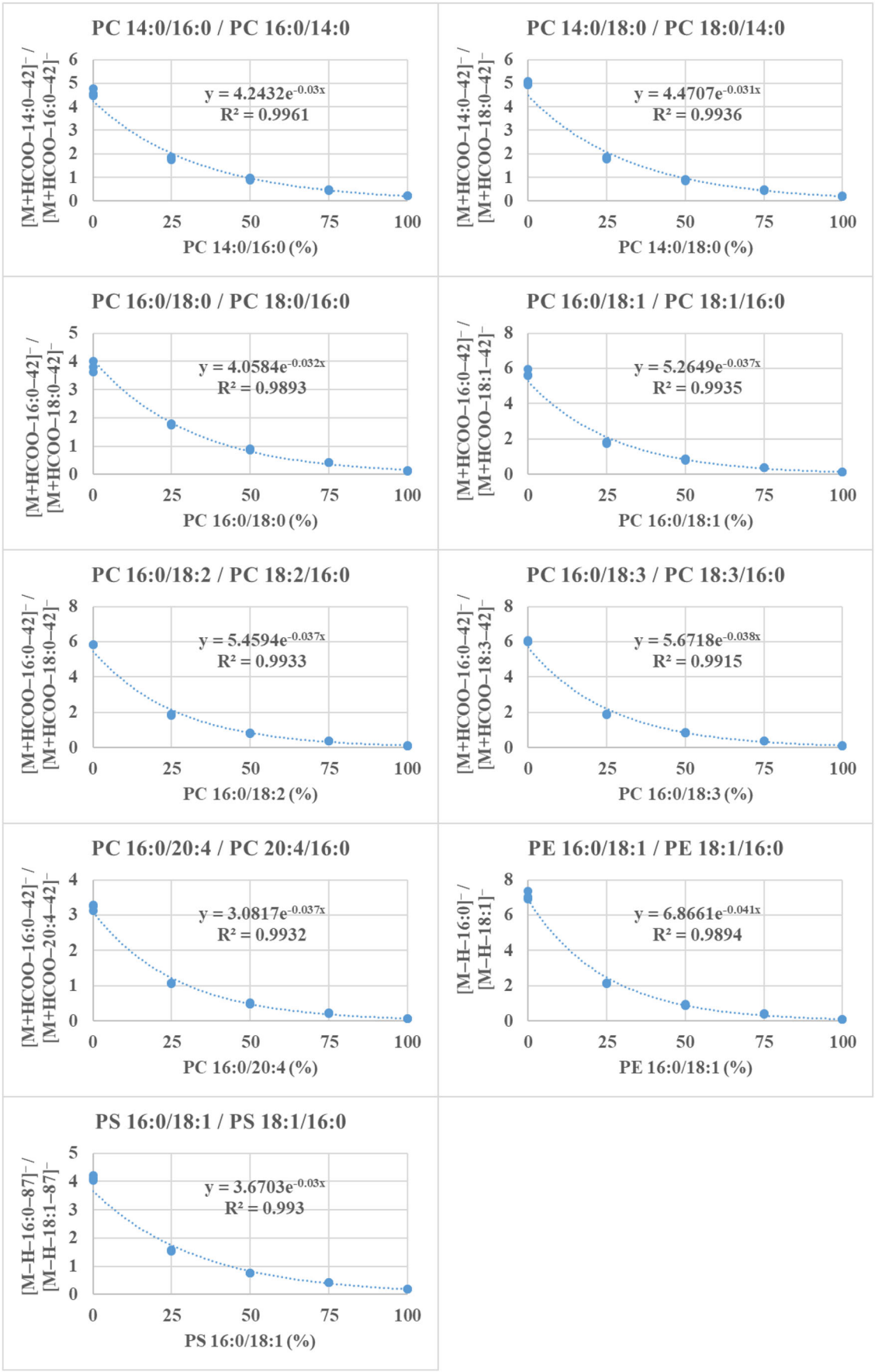


**FIGURE 5** Calibration curves of the regiospecific PL reference standards using the lysophospholipid-like fragment ion ratios

**TABLE 1** Results of individual regioisomer pair test mixtures obtained using the direct infusion method and a complex mixture of all reference standards obtained using the HILIC method

| Individual regioisomer pairs analyzed separately, 60/40% ratios, direct infusion method, MRM, n = 3 | | | | Complex mixture with all reference standard regioisomer pairs, 60/40% ratios, HILIC method, autoMS/MS, n = 3 | | | |
|---|---|---|---|---|---|---|---|
| PL composition | Actual regioisomer ratios (%) | Regioisomer ratios calculated using $[RCOO]^-$ ions (%) | Regioisomer ratios calculated using lysophospholipid-like ions (%) | PL composition | Actual regioisomer ratios (%) | Regioisomer ratios calculated using $[RCOO]^-$ ions (%) | Regioisomer ratios calculated using lysophospholipid-like ions (%) |
| | | $[RCOO]^-$ | $[M + HCOO-RCOOH-42]^-$ | | | $[RCOO]^-$ | $[M + HCOO-RCOOH-42]^-$ |
| PC 14:0/16:0 | 60 | 61.2 ± 1.1 | 59.4 ± 1.1 | PC 14:0/16:0 | 60 | 60.4 ± 1.4 | 59.9 ± 1.0 |
| PC 16:0/14:0 | 40 | 38.8 ± 1.1 | 40.6 ± 1.1 | PC 16:0/14:0 | 40 | 39.6 ± 1.4 | 40.1 ± 1.0 |
| PC 14:0/18:0 | 60 | 62.8 ± 1.6 | 61.5 ± 3.8 | PC 14:0/18:0 | 60 | 66.3 ± 2.7 | 63.0 ± 1.4 |
| PC 18:0/14:0 | 40 | 37.2 ± 1.6 | 38.5 ± 3.8 | PC 18:0/14:0 | 40 | 33.7 ± 2.7 | 37.0 ± 1.4 |
| PC 16:0/18:0 | 60 | 60.7 ± 1.2 | 62.9 ± 1.7 | PC 16:0/18:0 | 60 | 56.3 ± 1.7 | 58.4 ± 1.2 |
| PC 18:0/16:0 | 40 | 39.3 ± 1.2 | 37.1 ± 1.7 | PC 18:0/16:0 | 40 | 43.7 ± 1.7 | 41.6 ± 1.2 |
| PC 16:0/18:1 | 60 | 59.2 ± 0.7 | 63.6 ± 2.4 | PC 16:0/18:1 | 60 | 65.1 ± 0.3 | 69.8 ± 0.5 |
| PC 18:1/16:0 | 40 | 40.8 ± 0.7 | 36.4 ± 2.4 | PC 18:1/16:0 | 40 | 34.9 ± 0.3 | 30.2 ± 0.5 |
| PC 16:0/18:2 | 60 | 63.3 ± 1.8 | 61.7 ± 0.8 | PC 16:0/18:2 | 60 | n.d. | n.d. |
| PC 18:2/16:0 | 40 | 36.7 ± 1.8 | 38.3 ± 0.8 | PC 18:2/16:0 | 40 | n.d. | n.d. |
| PC 16:0/18:3 | 60 | 61.9 ± 2.2 | 58.6 ± 1.5 | PC 16:0/18:3 | 60 | n.d. | n.d. |
| PC 18:3/16:0 | 40 | 38.1 ± 2.2 | 41.4 ± 1.5 | PC 18:3/16:0 | 40 | n.d. | n.d. |
| PC 16:0/20:4 | 60 | 64.1 ± 1.7 | 62.2 ± 0.9 | PC 16:0/20:4 | 60 | 65.6 ± 0.7 | 61.8 ± 1.3 |
| PC 20:4/16:0 | 40 | 35.9 ± 1.7 | 37.8 ± 0.9 | PC 20:4/16:0 | 40 | 34.4 ± 0.7 | 38.2 ± 1.3 |
| | | $[RCOO]^-$ | $[M-H-RCOOH]^-$ | | | $[RCOO]^-$ | $[M-H-RCOOH]^-$ |
| PE 16:0/18:1 | 60 | 58.9 ± 0.9 | 59.4 ± 1.0 | PE 16:0/18:1 | 60 | 58.2 ± 0.6 | 57.7 ± 1.4 |
| PE 18:1/16:0 | 40 | 41.1 ± 0.9 | 40.6 ± 1.0 | PE 18:1/16:0 | 40 | 41.8 ± 0.6 | 42.3 ± 1.4 |
| | | $[RCOO]^-$ | $[M-H-RCOOH-87]^-$ | | | $[RCOO]^-$ | $[M-H-RCOOH-87]^-$ |
| PS 16:0/18:1 | 60 | 63.6 ± 1.4 | 64.1 ± 1.8 | PS 16:0/18:1 | 60 | 64.5 ± 1.2 | 62.5 ± 0.5 |
| PS 18:1/16:0 | 40 | 36.4 ± 1.4 | 35.9 ± 1.8 | PS 18:1/16:0 | 40 | 35.5 ± 1.2 | 37.5 ± 0.5 |

n.d. = not determined.

sensitivity was generally much lower than the sensitivity of $[RCOO]^-$ ions. This is just to demonstrate that the calculations can be done using also these fragment ions, but we will continue our further method development primarily with the $[RCOO]^-$ ions due to higher sensitivity.

### 3.3.2 | Analysis of reference standard mixtures

In order to test and validate the functionality of the calibration curves, a mixture of each regioisomer pair was prepared at 60/40% ratios. Each regioisomer pair was analyzed as an individual sample using direct infusion, and in a complex mixture containing all the reference standard pairs using the HILIC method. Reproducibility of the fragment ion ratios was good for both the direct infusion and HILIC methods. The quantification results for individual 60/40% regioisomer pairs were very close to the actual ratios using both sets of calibration curves (Table 1), but regioisomeric quantification of certain chromatographically overlapping compounds would require better accuracy for precursor ion isolation, which is not possible with the current instrumentation. The quadrupole responsible for the precursor ion selection is not capable of distinguishing ions ±2 Da apart. This poses some challenges with our current HILIC method, because in some cases the only difference between the compounds is one double bond, resulting in 2 Da mass difference. For example, in the test sample mixture of regiopure standards of phosphatidylcholines, PC 16:0/18:1/ PC 18:1/16:0, PC 16:0/18:2/PC 18:2/16:0 and PC 16:0/18:3/PC 18:3/16:0 were partially overlapping in the chromatogram. All these regioisomer pairs have a common 16:0 FA and they are 2 Da apart from each other, which causes distortions in the fragment ion ratios. Using another mass spectrometer with better precursor ion isolation capabilities would solve this challenge. Additionally, changing the chromatography to reversed phase would likely bypass the issue. With HILIC, most PL molecular species within one class are clustered relatively close to each other and some are partially overlapping with each other. Reversed-phase chromatography would separate the PL molecular species primarily based on the attached FAs, and according to our preliminary experiments, resulting in better chromatographic separation of the molecular species within a class.

## 4 | CONCLUSIONS

In the current study, we present a novel ESI-MS/MS method for analysis and quantification of regioisomers of phospholipids utilizing calibration curves obtained with pure reference standards. While there are still further improvements to be made, the method described herein shows that both the FA fragment ions and the lysophospholipid-like fragment ions can be used to determine the regioisomeric composition of glycerophospholipids. The calibration curves constructed using regiospecific reference compounds of PC, PE and PS showed excellent coefficiency and high reproducibility for accurate determination of PL regioisomer ratios. Establishing correction factors for the FA fragment ions is one of the next steps in our studies, which might help with finding patterns and rules behind the fragmentation and the effect of different FA combinations. This could allow us to extrapolate new calibration curves from the existing data for other PL compounds that we do not have the reference standards for. Further, the method provides characteristic fragment ions for determination of molecular species of sphingomyelins. Accuracy of the precursor ion isolation is a challenge that could be solved by changing chromatography from HILIC to reversed phase or using another mass spectrometer. With reversed-phase chromatography we would lose the clear separation of PL classes, but gain significantly better separation for molecular species within a class. All things considered, the method shows great promise and establishes a framework for PL regioisomer analysis. We will continue working on and improving this method into a routine method for analysis of PLs in natural samples.

## ACKNOWLEDGMENTS

This research was funded by the Academy of Finland (Chiral lipids in chiral nature: a novel strategy for regio- and stereospecific research of human milk and omega-3 lipids, decision No. 310982) and University of Turku Graduate School (Doctoral Programme in Molecular Life Sciences). Jukka-Pekka Suomela is thanked for critically reviewing the manuscript and for technical assistance with the mass spectrometer.

## CONFLICT OF INTEREST

Authors have declared no conflicts of interest.

## PEER REVIEW

The peer review history for this article is available at https://publons.com/publon/10.1002/rcm.9151.

## DATA AVAILABILITY STATEMENT

The data that support the findings of this study are available from the corresponding author upon reasonable request.

## ORCID

*Mikael Fabritius* https://orcid.org/0000-0003-4888-6587

*Baoru Yang* https://orcid.org/0000-0001-5561-514X

## REFERENCES

1. Snow DR, Jimenez-Flores R, Ward RE, et al. Dietary milk fat globule membrane reduces the incidence of aberrant crypt foci in Fischer-344 rats. *J Agric Food Chem*. 2010;58(4):2157-2163. https://doi.org/10.1021/jf903617q
2. Hossain Z, Hosokawa M, Takahashi K. Growth inhibition and induction of apoptosis of colon cancer cell lines by applying marine phospholipid. *Nutr Cancer*. 2009;61(1):123-130. https://doi.org/10.1080/01635580802395725
3. Fukunaga K, Hossain Z, Takahashi K. Marine phosphatidylcholine suppresses 1,2-dimethylhydrazine-induced colon carcinogenesis in rats by inducing apoptosis. *Nutr Res*. 2008;28(9):635-640. https://doi.org/10.1016/j.nutres.2008.05.005

4. Nagata T, Yaguchi T, Nishizaki T. DL- and PO-phosphatidylcholines as a promising learning and memory enhancer. *Lipids Health Dis*. 2011; 10(1):25. https://doi.org/10.1186/1476-511X-10-25
5. Konagai C, Yanagimoto K, Hayamizu K, Li H, Tsuji T, Koga Y. Effects of krill oil containing n-3 polyunsaturated fatty acids in phospholipid form on human brain function: A randomized controlled trial in healthy elderly volunteers. *Clin Interv Aging*. 2013;8:1247-1257. https://doi.org/10.2147/CIA.S50349
6. Cohn JS, Wat E, Kamili A, Tandy S. Dietary phospholipids, hepatic lipid metabolism and cardiovascular disease. *Curr Opin Lipidol*. 2008; 19(3):257-262. https://doi.org/10.1097/MOL.0b013e3282ffaf96
7. Berge K, Musa-Veloso K, Harwood M, Hoem N, Burri L. Krill oil supplementation lowers serum triglycerides without increasing low-density lipoprotein cholesterol in adults with borderline high or high triglyceride levels. *Nutr Res*. 2014;34(2):126-133. https://doi.org/10.1016/j.nutres.2013.12.003
8. Erös G, Ibrahim S, Siebert N, Boros M, Vollmar B. Oral phosphatidylcholine pretreatment alleviates the signs of experimental rheumatoid arthritis. *Arthritis Res Ther*. 2009;11(2):R43. https://doi.org/10.1186/ar2651
9. Miranda DTSZ, Batista VG, Grando FCC, et al. Soy lecithin supplementation alters macrophage phagocytosis and lymphocyte response to concanavalin A: A study in alloxan-induced diabetic rats. *Cell Biochem Funct*. 2008;26(8):859-865. https://doi.org/10.1002/cbf.1517
10. Kennedy K, Fewtrell MS, Morley R, et al. Double-blind, randomized trial of a synthetic triacylglycerol in formula-fed term infants: Effects on stool biochemistry, stool characteristics, and bone mineralization. *Am J Clin Nutr*. 1999;70(5):920-927. https://doi.org/10.1093/ajcn/70.5.920
11. Lasekan JB, Hustead DS, Masor M, Murray R. Impact of palm olein in infant formulas on stool consistency and frequency: A meta-analysis of randomized clinical trials. *Food Nutr Res*. 2017;61(1):1330104. https://doi.org/10.1080/16546628.2017.1330104
12. López-López A, Castellote-Bargalló AI, Campoy-Folgoso C, et al. The influence of dietary palmitic acid triacylglyceride position on the fatty acid, calcium and magnesium contents of at term newborn faeces. *Early Hum Dev*. 2001;65:S83-S94. https://doi.org/10.1016/S0378-3782(01)00210-9
13. Shoji H, Shimizu T, Kaneko N, et al. Comparison of the phospholipid classes in human milk in Japanese mothers of term and preterm infants. *Acta Paediatr*. 2006;95(8):996-1000. https://doi.org/10.1080/08035250600660933
14. Avalli A, Contarini G. Determination of phospholipids in dairy products by SPE/HPLC/ELSD. *J Chromatogr A*. 2005;1071(1–2): 185-190. https://doi.org/10.1016/j.chroma.2005.01.072
15. Donato P, Cacciola F, Cichello F, Russo M, Dugo P, Mondello L. Determination of phospholipids in milk samples by means of hydrophilic interaction liquid chromatography coupled to evaporative light scattering and mass spectrometry detection. *J Chromatogr A*. 2011;1218(37):6476-6482. https://doi.org/10.1016/j.chroma.2011.07.036
16. Liu ZY, Zhou DY, Zhao Q, et al. Characterization of glycerophospholipid molecular species in six species of edible clams by high-performance liquid chromatography-electrospray ionization-tandem mass spectrometry. *Food Chem*. 2017;219:419-427. https://doi.org/10.1016/j.foodchem.2016.09.160
17. Ali AH, Zou X, Lu J, et al. Identification of phospholipids classes and molecular species in different types of egg yolk by using UPLC-Q-TOF-MS. *Food Chem*. 2017;221:58-66. https://doi.org/10.1016/j.foodchem.2016.10.043
18. Viidanoja J. Analysis of phospholipids in bio-oils and fats by hydrophilic interaction liquid chromatography–tandem mass spectrometry. *J Chromatogr B Analyt Technol Biomed Life Sci*. 2015;1 (001):140-149. https://doi.org/10.1016/j.jchromb.2015.07.036
19. Song S, Cheong LZ, Wang H, et al. Characterization of phospholipid profiles in six kinds of nut using HILIC-ESI-IT-TOF-MS system. *Food Chem*. 2018;240:1171-1178. https://doi.org/10.1016/j.foodchem.2017.08.021
20. Gang KQ, Zhou DY, Lu T, et al. Direct infusion mass spectrometric identification of molecular species of glycerophospholipid in three species of edible whelk from Yellow Sea. *Food Chem*. 2018;245:53-60. https://doi.org/10.1016/j.foodchem.2017.10.077
21. Manicke NE, Wiseman JM, Ifa DR, Cooks RG. Desorption electrospray ionization (DESI) mass spectrometry and tandem mass spectrometry (MS/MS) of phospholipids and sphingolipids: Ionization, adduct formation, and fragmentation. *J Am Soc Mass Spectrom*. 2008;19(4):531-543. https://doi.org/10.1016/j.jasms.2007.12.003
22. Hvattum E, Hagelin G, Larsen Å. Study of mechanisms involved in the collision-induced dissociation of carboxylate anions from glycerophospholipids using negative ion electrospray tandem quadrupole mass spectrometry. *Rapid Commun Mass Spectrom*. 1998;12(19):1405-1409. https://doi.org/10.1002/(SICI)1,097-0231(19981015)12:19%3C1,405::AID-RCM338%3E3.0.CO;2-B
23. Larsen Å, Uran S, Jacobsen PB, Skotland T. Collision-induced dissociation of glycero phospholipids using electrospray ion-trap mass spectrometry. *Rapid Commun Mass Spectrom*. 2001;15(24): 2393-2398. https://doi.org/10.1002/rcm.520
24. Kerwin JL, Tuininga AR, Ericsson LH. Identification of molecular species of glycerophospholipids and sphingomyelin using electrospray mass spectrometry. *J Lipid Res*. 1994;35(6):1102-1114. https://doi.org/10.1016/S0022-2275(20)40106-3
25. Hsu F-F, Turk J. Electrospray ionization/tandem quadrupole mass spectrometric studies on phosphatidylcholines: The fragmentation processes. *J Am Soc Mass Spectrom*. 2003;14(4):352-363. https://doi.org/10.1016/S1044-0305(03)00064-3
26. Hsu F-F, Turk J. Studies on phosphatidylserine by tandem quadrupole and multiple stage quadrupole ion-trap mass spectrometry with electrospray ionization: Structural characterization and the fragmentation processes. *J Am Soc Mass Spectrom*. 2005;16(9): 1510-1522. https://doi.org/10.1016/j.jasms.2005.04.018
27. Hsu F-F, Turk J. Electrospray ionization with low-energy collisionally activated dissociation tandem mass spectrometry of glycerophospholipids: Mechanisms of fragmentation and structural characterization. *J Chromatogr B*. 2009;877(26):2673-2695. https://doi.org/10.1016/j.jchromb.2009.02.033
28. Hsu F-F, Turk J. Characterization of phosphatidylinositol, phosphatidylinositol-4-phosphate, and phosphatidylinositol-4,5-bisphosphate by electrospray ionization tandem mass spectrometry: A mechanistic study. *J Am Soc Mass Spectrom*. 2000;11 (11):986-999. https://doi.org/10.1016/S1044-0305(00)00172-0
29. Hsu F-F, Turk J. Charge-driven fragmentation processes in diacyl glycerophosphatidic acids upon low-energy collisional activation. A mechanistic proposal. *J Am Soc Mass Spectrom*. 2000;11(9):797-803. https://doi.org/10.1016/S1044-0305(00)00151-3
30. Hsu F-F, Turk J. Charge-remote and charge-driven fragmentation processes in diacyl glycerophosphoethanolamine upon low-energy collisional activation: A mechanistic proposal. *J Am Soc Mass Spectrom*. 2000;11(10):892-899. https://doi.org/10.1016/S1044-0305(00)00159-8
31. Taguchi R, Ishikawa M. Precise and global identification of phospholipid molecular species by an Orbitrap mass spectrometer and automated search engine Lipid Search. *J Chromatogr A*. 2010; 1217(25):4229-4239. https://doi.org/10.1016/j.chroma.2010.04.034
32. Aristizabal-Henao JJ, Fernandes MF, Duncan RE, Stark KD. Development of a rapid ultra high-performance liquid chromatography/tandem mass spectrometry method for the analysis of sn-1 and sn-2 lysophosphatidic acid regioisomers in mouse plasma. *Lipids*. 2019;54(8):479-486. https://doi.org/10.1002/lipd.12172

33. Nakanishi H, Iida Y, Shimizu T, Taguchi R. Separation and quantification of sn-1 and sn-2 fatty acid positional isomers in phosphatidylcholine by RPLC-ESIMS/MS. *J Biochem*. 2010;147(2):245-256. https://doi.org/10.1093/jb/mvp171
34. Wozny K, Lehmann WD, Wozny M, Akbulut BS, Brügger B. A method for the quantitative determination of glycerophospholipid regioisomers by UPLC-ESI-MS/MS. *Anal Bioanal Chem*. 2019;411(4):915-924. https://doi.org/10.1007/s00216-018-1,517-5
35. Baba T, Campbell JL, le Blanc JCY, Baker Paul RS, Ikeda K. Quantitative structural multiclass lipidomics using differential mobility: Electron impact excitation of ions from organics (EIEIO) mass spectrometry. *J Lipid Res*. 2018;59(5):910-919. https://doi.org/10.1194/jlr.D083261
36. Keller BO, Sui J, Young AB, Whittal RM. Interferences and contaminants encountered in modern mass spectrometry. *Anal Chim Acta*. 2008;627(1):71-81. https://doi.org/10.1016/j.aca.2008.04.043
37. Lísa M, Cífková E, Holčapek M. Lipidomic profiling of biological tissues using off-line two-dimensional high-performance liquid chromatography–mass spectrometry. *J Chromatogr A*. 2011;1218(31):5146-5156. https://doi.org/10.1016/j.chroma.2011.05.081
38. Han X, Gross RW. Structural determination of picomole amounts of phospholipids via electrospray ionization tandem mass spectrometry. *J Am Soc Mass Spectrom*. 1995;6(12):1202-1210. https://doi.org/10.1016/1044-0305(95)00568-4

## SUPPORTING INFORMATION

Additional supporting information may be found online in the Supporting Information section at the end of this article.

**How to cite this article:** Fabritius M, Yang B. Direct infusion and ultra-high-performance liquid chromatography/electrospray ionization tandem mass spectrometry analysis of phospholipid regioisomers. *Rapid Commun Mass Spectrom*. 2021;35(18):e9151. https://doi.org/10.1002/rcm.9151